Winds of Stars and Exoplanets
Proceedings IAU Symposium No. 370, 2023
A. A. Vidotto, L. Fossati & J. S. Vink, eds.
doi:10.1017/S1743921322004239

Observations of planetary winds and outflows

Leonardo A. Dos Santos

Space Telescope Science Institute, 3700 San Martin Drive, Baltimore, MD 21218, USA

Abstract. We have recently hit the milestone of 5,000 exoplanets discovered. In stark contrast with the Solar System, most of the exoplanets we know to date orbit extremely close to their host stars, causing them to lose copious amounts of gas through atmospheric escape at some stage in their lives. In some planets, this process can be so dramatic that they shrink in timescales of a few million to billions of years, imprinting features in the demographics of transiting exoplanets. Depending on the transit geometry, ionizing conditions, and atmospheric properties, a planetary outflow can be observed using transmission spectroscopy in the ultraviolet, optical or near-infrared. In this review, we will discuss the main techniques to observe evaporating exoplanets and their results. To date, we have evidence that at least 28 exoplanets are currently losing their atmospheres, and the literature has reported at least 42 non-detections.

Keywords. (stars:) planetary systems, planets and satellites: general, techniques: spectroscopic

1. Introduction

The discovery of 51 Peg b, a Jupiter-mass planet orbiting a Sun-like star with a period of only 4.3 days (Mayor & Queloz 1995), was initially received by the astronomical community with skepticism. But less than one year after this unexpected discovery, several other short-period gas giants were announced by competing teams (Schilling 1996), leading us to come to terms with these so-called "hot Jupiters" likely being a natural outcome of planet formation and evolution. One of the first questions that were posed during these early years of exoplanet science was whether hot Jupiters could survive the high mass loss rates driven by the extreme stellar irradiation at short periods (Guillot et al. 1996). The current consensus is that hot Jupiters are massive enough to retain their atmospheres for billions of years, but the same cannot be said about other hot exoplanets (e.g., Lecavelier Des Etangs 2007; Koskinen et al. 2007).

Hydrodynamic atmospheric escape was originally formulated by Watson et al. (1981) to explain the early evolution of the Earth and Venus. The idea behind this formulation stemmed from the insight of Gross (1972), who argued that, for planets with exospheres hotter than ∼10 000 K, a selective escape of gases (as in Öpik 1963) would be impossible. Instead, what follows is a bulk motion of gas in the upper atmosphere, or a so-called planetary outflow. More than two decades later, however, this process would be invoked to explain, at least partially, the observation of extended atmospheres in transiting exoplanets (e.g., Vidal-Madjar et al. 2003; Lecavelier des Etangs et al. 2010) and later some demographic features in the exoplanet population (e.g., Szabó & Kiss 2011; Owen & Wu 2013).

The main technique used to observe outflows in exoplanets is called transmission spectroscopy. This is the same method that yielded the first detection of sodium in an exoplanet (Charbonneau et al. 2002), and remains one of the most prolific techniques to study atmospheres in extrasolar worlds. When a planet transits, part of the host star's light is filtered through the thin layer of gas at the limbs of the planet, imprinting

wavelength-dependent signatures in the in-transit spectrum. This dependency emerges mainly due to a combination of the density, velocity, altitude and chemical composition of the absorbing material.

Tipically, the ratio of the area covered by the lower-atmosphere and the disk of a star is in the order of 10^{-3} to 10^{-4} in the optical and near-infrared (Seager & Sasselov 2000). This level of precision requires strong spectroscopic features to be detectable (e.g., Wyttenbach et al. 2015; Sing et al. 2016). At higher altitudes, where the atmosphere is gravitationally unbound from the planet, the diffuse gas can extend to several planetary radii and produce deep in-transit absorption signatures (e.g., Ehrenreich et al. 2015). It is precisely at high altitudes that we can observe signatures of planetary outflows.

This review has the following structure: In Sect. 2, we will discuss the basic formulation that serves as the backbone of the transit spectroscopy technique; in Sect. 3, we shall go over the main results of searches for escape of hydrogen using the Lyman-α and Balmer-series lines; in Sect. 4, we discuss the observations of exospheric metals, the smoking-gun signal of hydrodynamic escape in exoplanets; in Sect. 5, we will discuss metastable He transmission spectroscopy, currently the most productive technique to observe atmospheric escape; finally, in Sect. 6, we draw some of the main conclusions stemming from these observations and propose some new perspectives for future research in this sub-field of exoplanet science.

2. The basics of transit spectroscopy

In this manuscript, we shall adopt that the transmission spectrum ϕ of an exoplanet in function of transit phase θ and wavelength λ is given by:

$$\phi(\theta, \lambda) = 1 - \frac{f_{\rm in}(\theta, \lambda)}{F_{\rm out}(\lambda)}. \tag{2.1}$$

where $F_{\rm out}$ is the out-of-transit spectrum of the host star and $f_{\rm in}$ is the observed in-transit spectrum†. It is also convenient to define the transmission spectrum in the rest frame of the planet by Doppler shifting the spectra according to:

$$\lambda_{\rm p}(\theta) = \lambda \left(\frac{c}{\Delta v(\theta)} + 1 \right), \tag{2.2}$$

where Δv is the difference between radial velocity of the planet at a particular phase θ and the reference velocity of the observer, and $\lambda_{\rm p}$ will be the resulting wavelength in the rest frame of the planet. Finally, we can define the transmission spectrum Φ independent from the planetary phase by taking the mean of $\phi(\theta, \lambda_{\rm p})$ over the range of θ observed in transit:

$$\Phi(\lambda_{\rm p}) = \frac{1}{\Delta\theta} \int \phi(\theta, \lambda_{\rm p}) d\theta. \tag{2.3}$$

At low spectral resolution we cannot resolve the variation of the in-transit absorption with respect to the planetary Doppler velocity, and the transmission spectrum can be simplified to:

$$\Phi(\lambda) = 1 - \frac{F_{\rm in}(\lambda)}{F_{\rm out}(\lambda)}. \tag{2.4}$$

In the formulation described above, we averaged the in-transit signature over the phase space and study the signature in function of wavelength. As we will see in Sections 3 and 4, light curves are also routinely used to study transit spectra and search for in-transit

† We use lower-case f to denote the dependence of the in-transit spectra to the orbital phase θ. For the out-of-transit flux, we adopt upper-case F to indicate that it does not depend on the planetary phase.

https://doi.org/10.1017/S1743921322004239 Published online by Cambridge University Press

excess absorption that could indicate the presence of an atmosphere. In this method, we instead average signals over the wavelength space, and analyze its dependence in fuction of transit phase. As a recommendation for the reader, a more detailed treatise on transit spectroscopy can be found in Deming et al. (2021).

3. Escape of H: Lyman-α and Balmer-series spectroscopy

Classically, observations of atmospheric escape in exoplanets have been performed in ultraviolet (UV), which probes escape of hydrogen (H) and metallic species (see Sect. 4). The spectral feature of strongest interest is the Lyman-α (hereafter Lyα) line at 1215.67 Å, which traces atomic H. The *Hubble Space Telescope* (*HST*) is currently the only instrument capable of observing the Lyα, and it is possibly going to remain in this position until the launch of the next flagship NASA space telescope (National Academies of Sciences, Engineering, and Medicine 2021).

Since the interstellar medium (ISM) is rich in neutral H, the stellar Lyα line is partially or completely absorbed when observed from the Solar System. For stars with low radial velocities, the ISM absorption takes place near the core of the line; those with large radial velocities in relation to the Solar System and the ISM manage to dodge the absorption, and their Lyα cores are observable; see, e.g., the cases of Kepler-444 (Bourrier et al. 2017b) and Barnard's Star (France et al. 2020). Save a few exceptions, it is likely that the Lyα line is completely absorbed by the ISM for F, G and K-type stars beyond 60 pc; for M dwarfs, this limiting distance is much shorter.

Some other H features can be observed at optical wavelengths, such as the Balmer series (which include Hα, Hβ, Hγ), and provide another window to observe H escape in exoplanets. Observing in the optical has its advantages: there is no strict need to use a space telescope, ISM absorption is not a limiting issue, and it can be performed at high resolution. The disadvantages are that only highly-irradiated hot Jupiters display an in-transit absorption in the Balmer series, and no detection has so far been obtained for smaller or less irradiated planets (see Sect. 3.3).

3.1. *Hot Jupiters*

The first exoplanet to have a definitive detection of escaping H was the hot Jupiter HD 209458 b, as originally reported by Vidal-Madjar et al. (2003) and later confirmed by Ehrenreich et al. (2008). Using *HST* and the Space Telescope Imaging Spectrograph (STIS), Vidal-Madjar et al. (2003) detected a flux decrease of $15\% \pm 4\%$ in the blue wing of the Lyα line of the host star during the transit of the planet; since the transit depth at optical wavelengths is only $\sim 1.5\%$, the authors argued that the excess absorption seen in Lyα is due to a large cloud of H surrounding HD 209458 b, which in turn is fed by atmospheric escape.

One particular point of contention in the literature related to Lyα detections is regarding the Doppler velocities at which the signatures are measured; in the case of HD 209458 b, the in-transit planetary absorption takes place at velocities as high as -130 km s^{-1} in the stellar rest frame, indicating that the detected escaping material is accelerated away from the star. One-dimensional hydrodynamic escape models are unable to explain such high velocities (Murray-Clay et al. 2009), thus requiring other processes to explain them. The exact mechanism behind this effect has been the subject of an intense debate in the literature, and the most discussed contenders are radiation pressure and charge exchange in the interface between the stellar and planetary winds (e.g., Holmström et al. 2008; Lecavelier Des Etangs et al. 2008; Bourrier & Lecavelier des Etangs 2013; Vidotto & Bourrier 2017; Wang & Dai 2018; Debrecht et al. 2020).

https://doi.org/10.1017/S1743921322004239 Published online by Cambridge University Press

Using *HST*, but this time with the 1-st order CCD/G430M setup at optical wavelengths, Ballester et al. (2007) reported on an excess absorption of $0.03\% \pm 0.006\%$ during the transit of HD 209458 b. The authors argue that this feature is caused by a large population of hot H atoms in the planet's upper atmosphere, which absorb the stellar light in the Balmer jump and continuum.

Another early discovery of evaporation was that of the extensively studied hot Jupiter HD 189733 b (Lecavelier des Etangs et al. 2010), for which the authors detect an in-transit Lyα absorption of $14.4\% \pm 3.6\%$. Similar to HD 209458 b, this absorption takes place at highly blueshifted Doppler velocities. The main point of discussion for this planet is that there is strong evidence that its escape signals and its high-energy environment are variable (Lecavelier des Etangs et al. 2012; Bourrier et al. 2013, 2020; Pillitteri et al. 2022); as we shall see in the next sections, this variability has not only been observed in Lyα, but other wavelengths as well.

The search for escape of atomic H is complicated by the fact that they rely predominantly on *HST*, which is oversubscribed. However, excited H has been detected in the archetypal hot Jupiters HD 209458 b and HD 189733 b (Jensen et al. 2012), and in the ultra-hot Jupiter KELT-9 b (Yan & Henning 2018; Cauley et al. 2019; Wyttenbach et al. 2020; Sánchez-López et al. 2022) using the Balmer series H lines. Similar to the Lyα observations, HD 189733 b also displays signals of variability in the Hα line (Cauley et al. 2017a). Other hot Jupiters with reported Hα detections are WASP-12 b (Jensen et al. 2018), KELT-20 b (Casasayas-Barris et al. 2018), WASP-52 b (Chen et al. 2020), WASP-33 b (Yan et al. 2021b), and WASP-121 b (Yan et al. 2021a).

One of the main differences between the Lyα and Hα detections is that the latter tend to display excess in-transit absorption in the order of 1%, which is shallower than the former. Another key difference is that ISM absorption is not a limitation for these observations, and we have access to the core of the absorption. In fact, observations at high spectral resolution show that the excess in-transit signals in the Balmer series do not show a net blueshift, and are thus confined to relatively low Doppler velocities when compared to Lyα. From the modeling perspective, these low-velocity signatures are advantageous because they do not require expensive three-dimensional simulations. This, in turn, means that we can use simplified formulations to extract mass loss rates for the observed exoplanet, such as the Parker-wind (Parker 1958) approximation, as seen in Wyttenbach et al. (2020) and Yan et al. (2021b).

3.2. *Neptunes and sub-Neptunes*

Although the first observations of atmospheric escape in exoplanets were obtained for hot Jupiters, Ehrenreich et al. (2011) predicted that evaporating Neptune-sized worlds could not only be observed as well, but would show excess in-transit absorption just as deep as their larger counterparts. What they did not predict is that this signal could, in fact, be even larger than that. Upon observing the warm Neptune Gl 436 b (also known as GJ 436 b) with *HST*/STIS, Ehrenreich et al. (2015) found that the Lyα blue wing of the host star is obscured by a factor of $56.3\% \pm 3.5\%$ when the planet transits (see Fig. 1; see also Kulow et al. 2014). Such a signal can only be explained by the presence of a large cloud of atomic H around the planet, fed by an atmospheric escape rate in the order of 10^9 g s^{-1} and accelerated away from the star. Further observations would later show that Lyα transit of Gl 436 b is not only deep, but also extremely asymmetric and long (Lavie et al. 2017), stable across several years and observable with *HST*/COS (Dos Santos et al. 2019). Since then, Gl 436 b has become the archetypal evaporating Neptune, and its observations have been extensively used to test modeling frameworks for atmospheric escape (e.g., Bourrier et al. 2015, 2016; Kislyakova et al. 2019;

https://doi.org/10.1017/S1743921322004239 Published online by Cambridge University Press

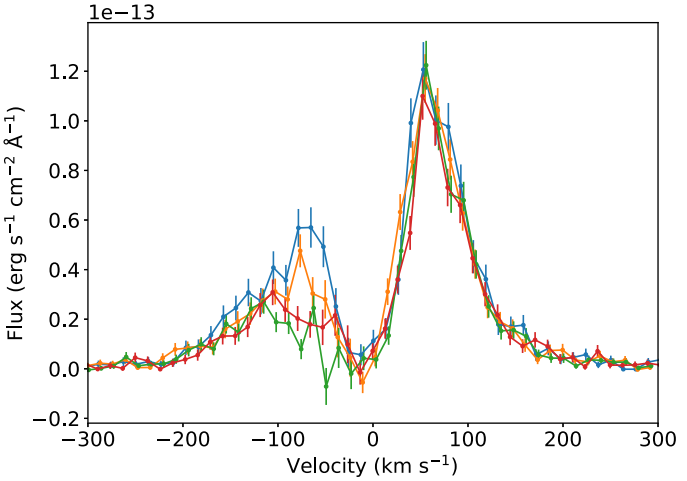

Figure 1. Lyman-α flux time-series during the transit of Gl 436 b, where blue and orange correspond to the spectra before the transit, green during the transit, and red after the transit (Ehrenreich et al. 2015). The deep absorption in the blue wing, between Doppler velocities [-120, -50] km s^{-1}, is explained by a large cloud of H around Gl 436 b fed by atmospheric escape.

Khodachenko et al. 2019; Villarreal D'Angelo et al. 2021; Attia et al. 2021; Carolan et al. 2021). Perhaps another warm Neptune that has become almost as iconic as Gl 436 b in the last few years is HAT-P-11 b, which displays signatures of atmospheric escape not only in Lyα (Ben-Jaffel et al. 2022), but also in ionized carbon and metastable helium (see Sections 4 and 5).

Similar escape signatures in other Neptunes have been observed in Lyα, and each of them stand out for a particular reason. GJ 3470 b was observed with *HST* in the Panchromatic Comparative Exoplanetology Treasury (PanCET) program with both the STIS and COS spectrographs (Bourrier et al. 2018b, 2021), yielding a signal of $35\% \pm 7\%$ in the blue wing, which is also explained by a large H exosphere similar to Gl 436 b. A key difference with GJ 3470 b is that it displays an in-transit excess absorption in the Lyα red wing as well, indicating the presence of material inflowing into the star. To this day, the exact physical mechanism behind this inflow remains a mystery, but Bourrier et al. (2018b) tentatively suggests that it could be caused by an elongated layer of dense atomic H extending beyond the Roche lobe. Using COS observations, Dos Santos et al. (2019) detected a similar, but episodic absorption in the red wing of Gl 436 during one of the observed transits of Gl 436 b in the PanCET program.

In this context, the tentative detection of exopsheric H in K2-18 b by Dos Santos et al. (2020b) stands out because this mini-Neptune is not, by any means, a hot exoplanet. Since it orbits an M dwarf with a period of approximately 30 days, K2-18 b is in fact a temperate world. The authors conclude that, due to how faint the host star is in the far-UV, more observations are necessary to confirm the detection. That notwithstanding, a primordial atmosphere of only a few percent mixing ratio of H can lead to temperatures in the upper atmosphere as high as 10 000 K, even in a temperate planet (Gross 1972). At these conditions, the kinetic energy of particles in the upper atmosphere exceed the gravitational potential of the planet, leading to a rapid atmospheric expansion and consequent escape. Furthermore, a recent study provided further support that planets at amenable levels of irradiation can sustain a large cloud of atomic H detectable during transits (Owen et al. 2021), but this hypothesis still requires further observations to be put under test. Another planet with a tentative Lyα detection is 55 Cnc b (Ehrenreich et al. 2012).

https://doi.org/10.1017/S1743921322004239 Published online by Cambridge University Press

Table 1. List of non-detections of H escape reported in the literature.

Planet name	Obs. method	Reference
HD 147506 b	Hα	Jensen et al. (2012)
HD 149026 b	Hα	Jensen et al. (2012)
HAT-P-32 b	Hα	Mallonn & Strassmeier (2016)
KELT-3 b	Hα	Cauley et al. (2017b)
Gl 436 b	Hα	Cauley et al. (2017b)
TRAPPIST-1 system	Lyα	Bourrier et al. (2017a)
Kepler-444 system	Lyα	Bourrier et al. (2017b)
HD 97658 b	Lyα	Bourrier et al. (2017c)
55 Cnc e	Lyα	Bourrier et al. (2018a)
GJ 1132 b	Lyα	Waalkes et al. (2019)
π Men c	Lyα	García Muñoz et al. (2020)
WASP-29 b	Lyα	Dos Santos et al. (2021)
K2-25 b	Lyα	Rockcliffe et al. (2021)
GJ 9827 b & d	Lyα and Hα	Carleo et al. (2021)
HD 63433 b	Lyα	Zhang et al. (2022d)

The case of the mini-Neptune HD 63433 c stands out for being the youngest transiting exoplanet with atmospheric escape detected in Lyα (Zhang et al. 2022d). It orbits a G5-type star with an orbital period of 20.5 d. Interestingly, the inner planet in the system, with a period of 7 d, does not display a Lyα signal, again providing support to the hypothesis that exospheric H in highly-irradiated Neptunes ionizes too quickly to be detectable in our observations. Similarly young exoplanets with signatures of evaporation are expected to be important to disentangle the roles of different escape mechanisms, such as photoevaporation and core-powered mass loss (e.g., Gupta & Schlichting 2020; King & Wheatley 2021). However, their observations are challenging due stellar activity modulation (Rackham et al. 2019, 2022), and even when detections have been observed, the interpretation can be complicated since their masses are usually not known (see, however, the case of K2-100 b in Barragán et al. 2019).

3.3. *Non-detections*

There are several reasons why atmospheric escape of H can remain undetected, even for planets that are expected to be evaporating. In Lyα, these reasons boil down to: (i) ISM absorption, which absorbs the flux at Doppler velocities where the absorption was supposed to take place; and ii) The host star luminosity yields a low signal-to-noise ratio, which is the usual suspect for M dwarfs. For Hα, the most likely limitation is the amount of ionized H in the atmosphere, which may not be high enough to produce a detectable signal.

Non-detections of atmospheric escape are severely under-reported, even though they can be just as informative as secure detections. In Table 1 we compile a list of non-detections of H escape that have been reported in refereed publications.

4. Hydrodynamic escape of metals observed in the UV

Other signatures of escape can be observed in UV wavelengths, among them the metal lines of carbon (C), nitrogen (N), oxygen (O), silicon (Si), magnesium (Mg), sulfur (S) and iron (Fe). Since these species are much heavier than H and He, they can only be lifted to the upper atmosphere when the escape is not selective; in other words, metals can only escape when the outflow is in a hydrodynamic regime. Similarly to Lyα, these metal lines are present in emission in stars of types between F and M. The advantage of observing these lines is that they do not have ISM absorption, or it is not as dramatic as in Lyα. The disadvantage is that metal lines are intrinsically weaker than Lyα, which means the detector will register lower count rates, yielding lower signal-to-noise ratios.

https://doi.org/10.1017/S1743921322004239 Published online by Cambridge University Press

For this reason, most of the detections of escaping metals have been obtained for hot Jupiters, where the signatures are stronger.

4.1. *Hot Jupiters*

Vidal-Madjar et al. (2004) first reported on the detection of O I and C II in the upper atmosphere of HD 209458 b using *HST*/STIS. According to the authors, the high velocity disperson and depth of the in-transit absorption suggests that the escaping metals are outflowing at supersonic velocities above the Roche lobe, an effect also known as geometric blow-off (Lecavelier des Etangs et al. 2004). In this Roche-lobe filling regime, the mass loss rates of hot exoplanets can be enhanced significantly; in the case of HD 209458 b, Erkaev et al. (2007) found this factor to be in the order of 50%. Using observations with the COS spectrograph, Linsky et al. (2010) reported on detections of C II and Si III in HD 209458 b, which is in conflict with the non-detection of Si III in Vidal-Madjar et al. (2004); however, these COS detections were later contested (Ballester & Ben-Jaffel 2015). Observations in the near-UV have yielded additional evidence for hydrodynamic escape in this planet associated with the presence of Mg I (Vidal-Madjar et al. 2013). According to the authors, the Mg feature probes the thermosphere and the exobase, precisely where the escape takes place; however, they also detect a tentative signal of a Mg comet-like tail in the exosphere of the planet. Finally, Schlawin et al. (2010) discussed a tentative detection of Si IV in the limb-brightened transit of HD 209458 b.

The archetypal hot Jupiter HD 189733 b was also among the early discoveries of escaping metals (Ben-Jaffel & Ballester 2013). Despite a significant stellar variability, the transit observations obtained with COS indicated the presence of O I and a possible early ingress associated with C II. HD 189733 b has since been observed again in the PanCET program, and the analysis of that dataset is currently under way.

Another category of planets that have become a testbed for atmospheric escape is that of the ultrahot Jupiters (UHJ), namely those that orbit closely to stars of type F or earlier. Because they orbit more massive stars, their escaping signatures are frequently detected in a regime of geometric blow-off. WASP-12 b was the first UHJ to have a detection of escaping metals. Using the COS spectrograph, Fossati et al. (2010) reported on excess in-transit absorption signatures in the core of the Mg II resonant lines at moderate significance, and on significantly enhanced transit depths measure in wide-band NUV light curves. The wide-band excess absorption are attributed to a collection of different absorbing metals in the exosphere of WASP-12 b.

The latest UHJ in which escaping metals have been detected is WASP-121 b (Sing et al. 2019). Based on STIS observations, the authors find evidence of Mg II and Fe II ions filling the Roche-lobe of the planet (see Fig. 2), and deeper broadband NUV light curves compared to optical wavelengths.

4.2. *Neptunes and sub-Neptunes*

To date, only two sub-Jovian worlds have been shown to display signatures of escaping metals, both of them obtained with *HST*/COS. The warm Neptune HAT-P-11 b has an excess in-transit absorption of $15\% \pm 4\%$ in the blue wing of the ground-state C II line at 133.45 nm, as well as a post-transit tail absorption of $12.5\% \pm 4\%$ (Ben-Jaffel et al. 2022). The authors argue that this signal is consistent with the planet's atmosphere having a sub-solar metallicity and an extended magnetotail.

The second, and perhaps most intriguing detection is that of the super-Earth π Men c (García Muñoz et al. 2021). Benefitting from the brightness of the host star, the authors reported on an in-transit absorption of $3.9\% \pm 1.1\%$ in the blue wing of the excited-state C II line at 1335 Å. Based on this single-transit observation, the authors concluded

https://doi.org/10.1017/S1743921322004239 Published online by Cambridge University Press

Table 2. List of non-detections of escaping metals reported in the literature.

Planet name	Instrument	Reference
WASP-13 b	*HST*/COS	Fossati et al. (2015)
55 Cnc e	Ground-based spectrographs	Ridden-Harper et al. (2016)
Gl 436 b	*HST*/STIS & COS	Loyd et al. (2017); Dos Santos et al. (2019)
WASP-18 b	*HST*/COS	Fossati et al. (2018)
WASP-29 b	*HST*/COS	Dos Santos et al. (2021)
HD 189733 b	XMM-Newton optical monitor	King et al. (2021)
GJ 3470 b	*HST*/COS	Bourrier et al. (2021)

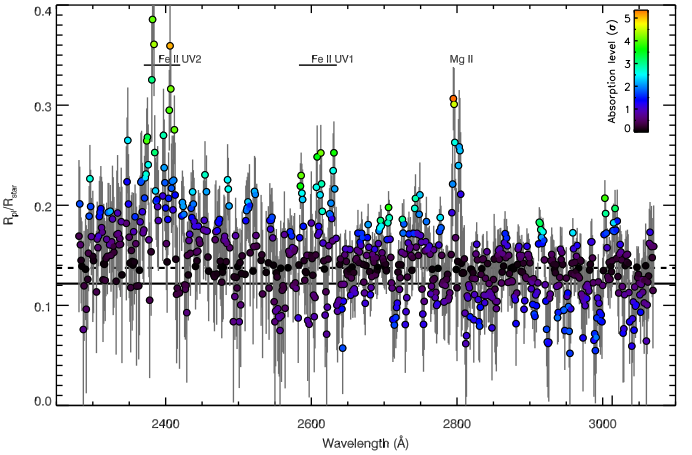

Figure 2. Transmission spectrum of WASP-121 b in the near-UV with detections of Mg II and Fe II (Sing et al. 2019). Reproduced with the permission of AAS Journals.

that π Men c possesses a thick atmosphere with more than 50% heavy volatiles in mass fraction, and that the escaping C fills the Roche lobe of the planet.

Although STIS observations hinted at a tentative detection of Si III in Gl 436 b (Lavie et al. 2017), an ensemble of COS data was later used to show that the observed signal was not present (Loyd et al. 2017), and that the STIS data was likely contaminated by stellar activity modulation (Dos Santos et al. 2019).

4.3. *Non-detections*

Similarly to Lyα, observations of metals in the UV suffer from the low signal-to-noise ratios, and this is probably the main limitation for transmission spectroscopy in these wavelengths. As seen in the case of π Men c (García Muñoz et al. 2021), some of the in-transit signals we are looking for are in the order of only a few percent, which requires high levels of contrast in order to be detected. Additionally, as shown by Dos Santos et al. (2019), stellar activity can also pose as a false positive. We list the non-detections of escaping metals reported in the literature in Table 2.

5. Metastable He spectroscopy in the near-infrared

Classically, the near-infrared helium (He) triplet located at 1.083 μm has been used to probe the chromosphere and transition region of cool stars (e.g., Andretta & Jones 1997). The presence of He in the upper atmospheres of exoplanets was originally predicted by the theoretical models of Seager & Sasselov (2000), but early observations of HD 209458 b were unable to detect a signal (Moutou et al. 2003). Several years later, Oklopčić & Hirata

https://doi.org/10.1017/S1743921322004239 Published online by Cambridge University Press

(2018) predicted that escaping He could produce signals as deep as 6% in the core of the triplet of HD 209458 b, which could be detectable at high spectral resolution.

Neutral He atoms can exist in two states: singlet (1^1S, electrons with anti-parallel spin) or triplet (2^3S, electrons with parallel spin). Since the radiative decay of triplet He into singlet state is relatively long, the former is also known as a metastable state. The formation of this line depends on the balance of rates that either populate or de-populate the triplet state: recombination, collisional excitation and de-excitation, charge exchange, and photoionization. According to Oklopčić (2019), planets orbiting late-type and active stars tend to display prominent in-transit He absorption due to their favorably high levels of extreme UV flux. Poppenhaeger (2022) further proposed that metastable He absorption also has a dependence on the iron abundance in the corona of stellar hosts, since most of the extreme-UV flux comes from coronal iron emission lines in cool stars. As we shall see shortly, this trend has mostly been held in our observations.

The most important advantage of observing metastable He is that this technique does not necessarilly require a space telescope, and can be observed from the ground. In fact, ground-based facilities can perform experiments at much higher spectral resolutions that those achieved from space. In this regime, the Doppler anomaly of the planet can be resolved during the transit (e.g., Wyttenbach et al. 2015), which helps in discerning if the signal is of planetary nature or stellar. As opposed to Lyα observations, the in-transit absorption is seen in the core and wings of the He triplet, which means we are not only probing the accelerated particles well above the exobase, but also the outflowing gas near the thermosphere. This allows us to use simpler, one-dimensional models to interpret the observations (e.g., Oklopčić & Hirata 2018; Lampón et al. 2020; Dos Santos et al. 2022; Linssen et al. 2022) and extract more precise mass loss rates than those determined from Lyα data (e.g., Bourrier & Lecavelier des Etangs 2013). The disadvantage of ground-based He spectroscopy is that, due to spectral normalization, information about the planetary continuum absorption is lost, but since the signals are relatively deep, the impact of this limitation is not of great importance. Other disadvantages include telluric contamination and lower sensitivities than space telescopes.

5.1. *Hot Jupiters*

For a change, the first discovery of metastable He in exoplanet was not in HD 209458 b, but rather the hot Jupiter WASP-107 b (Spake et al. 2018). In this study, the authors observed a single transit with *HST* and the Wide-Field Camera 3 (WFC3) instrument and measured a transit depth of $0.049\% \pm 0.011\%$ in a low-resolution bandpass of 98 Å. Later, this feature would be observed again from the ground and at high spectral resolution with the CARMENES spectrograph installed on the 3.5 m telescope at the Calar Alto Observatory (Allart et al. 2019) and with the Keck II/NIRSPEC spectrograph (Kirk et al. 2020). Recently, Spake et al. (2021) reported on the observation of the He tail that trails WASP-107 b, also detected with the NIRSPEC instrument.

Several other hot Jupiters have since been observed to be evaporating and exhibit in-transit He absorption. The CARMENES spectrograph has been particularly productive, yielding detections for HD 189733 b (with variability; Salz et al. 2018), WASP-69 b (Nortmann et al. 2018), HD 209458 b (Alonso-Floriano et al. 2019), HAT-P-32 b (Czesla et al. 2022) and a tentative detection for the UHJ WASP-76 b (Casasayas-Barris et al. 2021). Another productive instrument for He spectroscopy in hot Jupiters has been the NIRSPEC spectrograph, which was responsible for detections in HD 198733 b (Zhang et al. 2022a), WASP-52 b and a tentative signal for WASP-177 b (Kirk et al. 2022). Using the GIANO spectrograph installed on the Telescopio Nazionale Galileo (TNG), Guilluy et al. (2020) reproduced the He signature of HD 189733 b.

https://doi.org/10.1017/S1743921322004239 Published online by Cambridge University Press

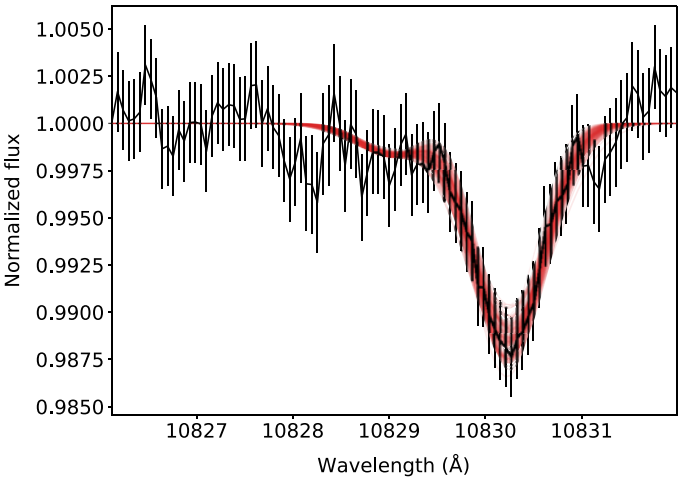

Figure 3. Transmission spectrum of HAT-P-11 b near the metastable He triplet observed with the CARMENES spectrograph (black symbols; Allart et al. 2018) and a family of transmission spectra simulations that were fit to the data based on an isothermal Parker-wind model (red curves; Dos Santos et al. 2022).

Following up on the increasing interest in atmospheric escape in exoplanets, Vissapragada et al. (2020) presented the first results detections of He using a new method: ultra-narrowband photometry of the He triplet with the Wide-field Infrared Camera (WIRC) installed on the 200-inch Hale Telescope at Palomar Observatory. They use a custom-made filter centered on 1083.3 nm in vacuum, with an FWHM of 0.635 nm, and a maximum transmission of 95.6%. Naturally, since measurements are performed in photometry, the in-transit absorption is not spectrally resolved, so the results do not encode information about velocities. However, the instrument has demonstrated a significant productivity, yielding detections for the hot Jupiters WASP-69 b (Vissapragada et al. 2020), HAT-P-18 b (Paragas et al. 2021), and tentative detections for WASP-52 b and NGTS-5 b (Vissapragada et al. 2022). This tentative observation for WASP-52 b, with an in-transit depth of $0.29\% \pm 0.13\%$ in the filter's bandpass, is in slight tension with the firm detection reported in Kirk et al. (2022), for which an in-transit depth of $0.66\% \pm 0.14\%$ was measured.

5.2. *Neptunes and sub-Neptunes*

The first reports of He observations in transiting hot Jupiters were concomitant with the discoveries in sub-Jovian worlds. Similar to Lyα results we listed in Sect. 3, Neptunes can also display deep in-transit signals that sometimes rival those of their larger counterparts. Using an *HST*/WFC3 archival dataset, Mansfield et al. (2018) demonstrated that the warm Neptune HAT-P-11 b has a transit depth of $\sim 0.355\%$ in a 49 Å-wide channel centered in the He triplet. This study was simultaneous to that of Allart et al. (2018), who reported a detection of He in HAT-P-11 b obtained with the CARMENES spectrograph. At high spectral resolution, this signature is resolved with an average depth of $1.08\% \pm 0.05\%$ (see Fig. 3).

Along with HAT-P-11 b, another warm Neptune to have both Lyα and He detections is GJ 3470 b (Ninan et al. 2020), the latter obtained with the Habitable Zone Planet Finder (HPF) spectrograph installed on the Hobby-Eberly Telescope (HET). This signal was also measured with CARMENES (Palle et al. 2020), and a large mass loss rate of $\sim 10^{11}$ g s^{-1} was inferred. Based on this observation, Lampón et al. (2021) concludes that

https://doi.org/10.1017/S1743921322004239 Published online by Cambridge University Press

Table 3. List of non-detections of metastable He reported in the literature.

Planet name	Instrument	Reference
HD 209458 b†	VLT/ISAAC	Moutou et al. (2003)
Gl 436 b	CAO 3.5m/CARMENES	Nortmann et al. (2018)
KELT-9 b	CAO 3.5m/CARMENES	Nortmann et al. (2018)
WASP-12 b	*HST*/WFC3	Kreidberg & Oklopčić (2018)
WASP-52 b†	Palomar/WIRC	Vissapragada et al. (2020)
K2-100 b	Subaru/IRD	Gaidos et al. (2020)
WASP-127 b	Gemini/Phoenix	Dos Santos et al. (2020a)
AU Mic b	Subaru/IRD & Keck II/NIRSPEC	Hirano et al. (2020)
GJ 1214 b†	Keck II/NIRSPEC	Kasper et al. (2020); Spake et al. (2022)
HD 97658 b	Keck II/NIRSPEC	Kasper et al. (2020)
55 Cnc e	Keck II/NIRSPEC	Zhang et al. (2021)
TRAPPIST-1 system	Subaru/IRD & HET/HPF	Krishnamurthy et al. (2021)
K2-136 c	Subaru/IRD	Gaidos et al. (2021)
V1298 Tau b & c	Palomar/WIRC	Vissapragada et al. (2021)
WASP-80 b	TNG/GIANO & Palomar/WIRC	Fossati et al. (2022), Vissapragada et al. (2022)
GJ 9827 d	Keck II/NIRSPEC	Kasper et al. (2020)
τ Boo b (in emission)	CAO 3.5m/CARMENES	Zhang et al. (2020)
GJ 9827 b & d	CAO 3.5m/CARMENES	Carleo et al. (2021)
HD 63433 system	Keck II/NIRSPEC	Zhang et al. (2022d)
WASP-177 b†	Palomar/WIRC	Vissapragada et al. (2022)

Notes: The † symbol denotes planets with alternate results that yielded a detection.

GJ 3470 b is in a photon-limited escape regime, where the mass loss rate is limited by the incident flux of ionizing photons (Owen & Alvarez 2016).

Using the NIRSPEC spectrograph, Kasper et al. (2020) concluded that the sub-Neptune GJ 1214 b does not have a detectable He signature. However, the observation of one transit with the CARMENES spectrograph reported by Orell-Miquel et al. (2022) yielded a tentative detection. According to Orell-Miquel et al., stellar activity alone cannot have caused a false-positive, and argue that telluric contamination is the probable culprit of the non-detection observed by Kasper et al.. This argument was further contested by Spake et al. (2022), who observed an additional NIRSPEC transit in an epoch of minimal telluric contamination and still obtained a non-detection.

The Palomar/WIRC narrowband photometry has proven to be precise enough to detect He outflows in Neptunes as well, with a firm detection for HAT-P-26 b (Vissapragada et al. 2022) and a tentative detection for the young sub-Neptune V1298 Tau d (Vissapragada et al. 2021). Young sub-Neptunes are target of strong importance for atmospheric escape observations because we think it is in their youth that most of photoevaporation takes place (e.g., Owen & Wu 2013). Using the NIRSPEC spectrograph, Zhang et al. (2022c,b) reported on the first discoveries of atmospheric escape in the young mini-Neptunes HD 73583 b, TOI-1430 b, TOI-2076 b and TOI-1683 b.

5.3. *Non-detections*

Many more planets than those listed in this review have been observed in He spectroscopy (priv. comm.), and the data analyses are currently under way. We list all the reported He non-detections in Table 3, where we also include those that have been positively detected using different instruments or analyses (these cases are marked with the symbol †).

6. Conclusions and future perspectives

Atmospheric escape has been studied in the Solar System since the beginning of the 20th Century. However, observations of upper atmospheres in hot exoplanets in the last

https://doi.org/10.1017/S1743921322004239 Published online by Cambridge University Press

Table 4. List of planets with detections of atmospheric escape.

Planet name	Signature(s)
HD 209458 b	Lyα, Balmer-series, metals, He
HD 189733 b	Lyα, Balmer-series, metals, He
KELT-9 b	Balmer-series
WASP-12 b	Balmer-series, metals
KELT-20 b	Balmer-series
WASP-52 b	Balmer-series, He
WASP-33 b	Balmer-series
WASP-121 b	Balmer-series, metals
Gl 436 b	Lyα
GJ 3470 b	Lyα, He
K2-18 b	Lyα (tentative)
HD 63433 c	Lyα
HAT-P-11 b	Lyα, C II, He
π Men c	C II
WASP-107 b	He
WASP-69 b	He
HAT-P-32 b	He
WASP-76 b	He (tentative)
WASP-177 b	He (tentative)
GJ 1214 b	He (tentative)
HAT-P-18 b	He
NGTS-5 b	He (tentative)
HAT-P-26 b	He
V1298 Tau d	He (tentative)
HD 73583 b	He
TOI-1430 b	He
TOI-2076 b	He
TOI-1683 b	He

two decades have advanced our understanding about the physics of evaporation by leaps and bounds. To date, we have observed escape in 28 exoplanets, including tentative detections (see a complete list in Table 4). These worlds have sizes varying from Jupiter-size to mini-Neptunes, and irradiation levels ranging from the most extremely-irradiated planet known (KELT-9 b) to Earth-like bolometric fluxes (K2-18 b).

Our observational efforts have shown that, so far, metastable He spectroscopy is the most productive avenue to observe escape in hot exoplanets with a H-dominated atmosphere orbiting active stars. Lyα observations, on the other hand, seem to yield detections for planets in relatively milder irradiation conditions. According to Owen et al. (2021), the reason for that is due to lack of observable flux in the core of the Lyα line, which means that we have access only to signatures that occur at high Doppler velocities. In order for H atoms to achieve these high velocities, they need to stay neutral for a long time and produce a detectable exospheric tail. For the cases where H ionizes too quickly in the exosphere, it is thus recommended to observe in the Balmer series lines. Some hot Jupiters, like HD 209458 b and HD 189733 b, have an optimal set of parameters that allows the detection of Lyα, He, Hα, and metals. Some Neptunes, like GJ 3470 b and HAT-P-11 b, also possess an optimal set of parameters that enables the observation of escape in more than one spectral channel. These cases seem to be, however, rare.

Despite these observational efforts, many questions related to the atmospheric evolution of exoplanets remain open. For instance, what are the mechanisms that carve the hot Neptune desert (e.g., Davis & Wheatley 2009; Szabó & Kiss 2011; Mazeh et al. 2016)? Based on a survey of escaping He in Saturn-sized ho gas giants with Palomar/WIRC, Vissapragada et al. (2022) concluded that the upper edge of the Neptune desert is stable against evaporation, with measured escape rates that remove less than 10% of these planet's masses. This suggests that other, additional mechanisms are necessary to carve the desert, such as a history of migration (e.g., Owen & Lai 2018; Attia et al. 2021).

https://doi.org/10.1017/S1743921322004239 Published online by Cambridge University Press

More observations and modeling are required to test these hypotheses. Another persistent open question in this field is whether close-in gas giant exoplanets have hydrodynamically unstable thermospheres (Salz et al. 2016), which was originally proposed by Watson et al. (1981) and confirmed for only a handful of exoplanets to date. More observations of exospheric metals will help elucidate this puzzle, since they trace hydrodynamic escape directly.

For the future, as we mentioned in Sect. 5, observing escape in young sub-Neptunes will also be important because it may give us clues about the respective roles of photoevaporation (driven by X-rays and extreme-UV irradiation; e.g., Lammer et al. 2003; Volkov et al. 2011; Tripathi et al. 2015; Erkaev et al. 2016) and core-powered mass loss (e.g., Ginzburg et al. 2018; Gupta & Schlichting 2019). The main challenge in this endeavor is that young stars are active, and the activity poses a problem to measure planetary masses through the radial velocity method and, in addition, can produce false-positive detections of escape (e.g., Dos Santos et al. 2019).

With a sample of 28 exoplanets with signals of atmospheric escape, we have by now gathered a sample with which we can begin interpreting at a comparative level. In order to answer some of the open questions described above, we will benefit from carrying out a uniform analysis of this sample with a common theoretical framework (see, e.g., Sing et al. 2016). To cite an example, this approach will enable us to find correlations between measured properties of evaporating exoplanets, such as their bulk density, incoming high-energy flux, and mass-loss rates (as predicted by the energy-limited formulation). Studies that have already begun performing this comparative exoplanetology approach for evaporating exoplanets are Lampón et al. (2021) and Vissapragada et al. (2022).

Finally, with the successful launch and commissioning of *JWST*, we will have yet another instrument capable of observing the metastable He line, and with space-based precision. Although its capabilities for He transmission spectroscopy remain to be tested, it has three instrument configurations that can measure spectra at 1.083 μm: NIRISS/SOSS (2nd order only), NIRSpec/G140M and NIRSpec/G140H. The downside of *JWST* is that its lower resolution may not be able to spectrally resolve the in-transit absorption, but a more precise instrument could enable us to observe fainter signatures than those accessible from the ground.

References

Allart, R., Bourrier, V., Lovis, C., et al. 2019, A&A, 623, A58
Allart, R., Bourrier, V., Lovis, C., et al. 2018, Science, 362, 1384
Alonso-Floriano, F. J., Snellen, I. A. G., Czesla, S., et al. 2019, A&A, 629, A110
Andretta, V. & Jones, H. P. 1997, ApJ, 489, 375
Attia, O., Bourrier, V., Eggenberger, P., et al. 2021, A&A, 647, A40
Ballester, G. E. & Ben-Jaffel, L. 2015, ApJ, 804, 116
Ballester, G. E., Sing, D. K., & Herbert, F. 2007, Nature, 445, 511
Barragán, O., Aigrain, S., Kubyshkina, D., et al. 2019, MNRAS, 490, 698
Ben-Jaffel, L. & Ballester, G. E. 2013, A&A, 553, A52
Ben-Jaffel, L., Ballester, G. E., García Muñoz, A., et al. 2022, Nature Astronomy, 6, 141
Bourrier, V., de Wit, J., Bolmont, E., et al. 2017a, AJ, 154, 121
Bourrier, V., Dos Santos, L. A., Sanz-Forcada, J., et al. 2021, A&A, 650, A73
Bourrier, V., Ehrenreich, D., Allart, R., et al. 2017b, A&A, 602, A106
Bourrier, V., Ehrenreich, D., King, G., et al. 2017c, A&A, 597, A26
Bourrier, V., Ehrenreich, D., & Lecavelier des Etangs, A. 2015, A&A, 582, A65
Bourrier, V., Ehrenreich, D., Lecavelier des Etangs, A., et al. 2018a, A&A, 615, A117
Bourrier, V. & Lecavelier des Etangs, A. 2013, A&A, 557, A124
Bourrier, V., Lecavelier des Etangs, A., Dupuy, H., et al. 2013, A&A, 551, A63
Bourrier, V., Lecavelier des Etangs, A., Ehrenreich, D., et al. 2018b, A&A, 620, A147

https://doi.org/10.1017/S1743921322004239 Published online by Cambridge University Press

Bourrier, V., Lecavelier des Etangs, A., Ehrenreich, D., Tanaka, Y. A., & Vidotto, A. A. 2016, A&A, 591, A121
Bourrier, V., Wheatley, P. J., Lecavelier des Etangs, A., et al. 2020, MNRAS, 493, 559
Carleo, I., Youngblood, A., Redfield, S., et al. 2021, AJ, 161, 136
Carolan, S., Vidotto, A. A., Villarreal D'Angelo, C., & Hazra, G. 2021, MNRAS, 500, 3382
Casasayas-Barris, N., Orell-Miquel, J., Stangret, M., et al. 2021, A&A, 654, A163
Casasayas-Barris, N., Pallé, E., Yan, F., et al. 2018, A&A, 616, A151
Cauley, P. W., Redfield, S., & Jensen, A. G. 2017a, AJ, 153, 217
Cauley, P. W., Redfield, S., & Jensen, A. G. 2017b, AJ, 153, 81
Cauley, P. W., Shkolnik, E. L., Ilyin, I., et al. 2019, AJ, 157, 69
Charbonneau, D., Brown, T. M., Noyes, R. W., & Gilliland, R. L. 2002, ApJ, 568, 377
Chen, G., Casasayas-Barris, N., Pallé, E., et al. 2020, A&A, 635, A171
Czesla, S., Lampón, M., Sanz-Forcada, J., et al. 2022, A&A, 657, A6
Davis, T. A. & Wheatley, P. J. 2009, MNRAS, 396, 1012
Debrecht, A., Carroll-Nellenback, J., Frank, A., et al. 2020, MNRAS, 493, 1292
Deming, D., Stevenson, K. B., & Ehrenreich, D. 2021, in ExoFrontiers; Big Questions in Exoplanetary Science, ed. N. Madhusudhan, 7–1
Dos Santos, L. A., Bourrier, V., Ehrenreich, D., et al. 2021, A&A, 649, A40
Dos Santos, L. A., Ehrenreich, D., Bourrier, V., et al. 2020a, A&A, 640, A29
Dos Santos, L. A., Ehrenreich, D., Bourrier, V., et al. 2020b, A&A, 634, L4
Dos Santos, L. A., Ehrenreich, D., Bourrier, V., et al. 2019, A&A, 629, A47
Dos Santos, L. A., Vidotto, A. A., Vissapragada, S., et al. 2022, A&A, 659, A62
Ehrenreich, D., Bourrier, V., Bonfils, X., et al. 2012, A&A, 547, A18
Ehrenreich, D., Bourrier, V., Wheatley, P. J., et al. 2015, Nature, 522, 459
Ehrenreich, D., Lecavelier Des Etangs, A., & Delfosse, X. 2011, A&A, 529, A80
Ehrenreich, D., Lecavelier Des Etangs, A., Hébrard, G., et al. 2008, A&A, 483, 933
Erkaev, N. V., Kulikov, Y. N., Lammer, H., et al. 2007, A&A, 472, 329
Erkaev, N. V., Lammer, H., Odert, P., et al. 2016, MNRAS, 460, 1300
Fossati, L., France, K., Koskinen, T., et al. 2015, ApJ, 815, 118
Fossati, L., Guilluy, G., Shaikhislamov, I. F., et al. 2022, A&A, 658, A136
Fossati, L., Haswell, C. A., Froning, C. S., et al. 2010, ApJ Letters, 714, L222
Fossati, L., Koskinen, T., France, K., et al. 2018, AJ, 155, 113
France, K., Duvvuri, G., Egan, H., et al. 2020, AJ, 160, 237
Gaidos, E., Hirano, T., Mann, A. W., et al. 2020, MNRAS, 495, 650
Gaidos, E., Hirano, T., Omiya, M., et al. 2021, Research Notes of the American Astronomical Society, 5, 238
García Muñoz, A., Fossati, L., Youngblood, A., et al. 2021, ApJ Letters, 907, L36
García Muñoz, A., Youngblood, A., Fossati, L., et al. 2020, ApJ Letters, 888, L21
Ginzburg, S., Schlichting, H. E., & Sari, R. 2018, MNRAS, 476, 759
Gross, S. H. 1972, Journal of Atmospheric Sciences, 29, 214
Guillot, T., Burrows, A., Hubbard, W. B., Lunine, J. I., & Saumon, D. 1996, ApJ Letters, 459, L35
Guilluy, G., Andretta, V., Borsa, F., et al. 2020, A&A, 639, A49
Gupta, A. & Schlichting, H. E. 2019, MNRAS, 487, 24
Gupta, A. & Schlichting, H. E. 2020, MNRAS, 493, 792
Hirano, T., Krishnamurthy, V., Gaidos, E., et al. 2020, ApJ Letters, 899, L13
Holmström, M., Ekenbäck, A., Selsis, F., et al. 2008, Nature, 451, 970
Jensen, A. G., Cauley, P. W., Redfield, S., Cochran, W. D., & Endl, M. 2018, AJ, 156, 154
Jensen, A. G., Redfield, S., Endl, M., et al. 2012, ApJ, 751, 86
Kasper, D., Bean, J. L., Oklopčić, A., et al. 2020, AJ, 160, 258
Khodachenko, M. L., Shaikhislamov, I. F., Lammer, H., et al. 2019, ApJ, 885, 67
King, G. W., Corrales, L., Wheatley, P. J., et al. 2021, MNRAS, 506, 2453
King, G. W. & Wheatley, P. J. 2021, MNRAS, 501, L28
Kirk, J., Alam, M. K., López-Morales, M., & Zeng, L. 2020, AJ, 159, 115

Kirk, J., Dos Santos, L. A., López-Morales, M., et al. 2022, AJ, 164, 24
Kislyakova, K. G., Holmström, M., Odert, P., et al. 2019, A&A, 623, A131
Koskinen, T. T., Aylward, A. D., & Miller, S. 2007, Nature, 450, 845
Kreidberg, L. & Oklopčić, A. 2018, Research Notes of the American Astronomical Society, 2, 44
Krishnamurthy, V., Hirano, T., Stefánsson, G., et al. 2021, AJ, 162, 82
Kulow, J. R., France, K., Linsky, J., & Loyd, R. O. P. 2014, ApJ, 786, 132
Lammer, H., Selsis, F., Ribas, I., et al. 2003, ApJ Letters, 598, L121
Lampón, M., López-Puertas, M., Czesla, S., et al. 2021, A&A, 648, L7
Lampón, M., López-Puertas, M., Lara, L. M., et al. 2020, A&A, 636, A13
Lavie, B., Ehrenreich, D., Bourrier, V., et al. 2017, A&A, 605, L7
Lecavelier Des Etangs, A. 2007, A&A, 461, 1185
Lecavelier des Etangs, A., Bourrier, V., Wheatley, P. J., et al. 2012, A&A, 543, L4
Lecavelier des Etangs, A., Ehrenreich, D., Vidal-Madjar, A., et al. 2010, A&A, 514, A72
Lecavelier Des Etangs, A., Vidal-Madjar, A., & Desert, J. M. 2008, Nature, 456, E1
Lecavelier des Etangs, A., Vidal-Madjar, A., McConnell, J. C., & Hébrard, G. 2004, A&A, 418, L1
Linsky, J. L., Yang, H., France, K., et al. 2010, ApJ, 717, 1291
Linssen, D., Oklopčić, A., & MacLeod, M. 2022, arXiv e-prints, arXiv:2209.03677
Loyd, R. O. P., Koskinen, T. T., France, K., Schneider, C., & Redfield, S. 2017, ApJ Letters, 834, L17
Mallonn, M. & Strassmeier, K. G. 2016, A&A, 590, A100
Mansfield, M., Bean, J. L., Oklopčić, A., et al. 2018, ApJ Letters, 868, L34
Mayor, M. & Queloz, D. 1995, Nature, 378, 355
Mazeh, T., Holczer, T., & Faigler, S. 2016, A&A, 589, A75
Moutou, C., Coustenis, A., Schneider, J., Queloz, D., & Mayor, M. 2003, A&A, 405, 341
Murray-Clay, R. A., Chiang, E. I., & Murray, N. 2009, ApJ, 693, 23
National Academies of Sciences, Engineering, and Medicine. 2021, Pathways to Discovery in Astronomy and Astrophysics for the 2020s (Washington, DC: The National Academies Press)
Ninan, J. P., Stefansson, G., Mahadevan, S., et al. 2020, ApJ, 894, 97
Nortmann, L., Pallé, E., Salz, M., et al. 2018, Science, 362, 1388
Oklopčić, A. 2019, ApJ, 881, 133
Oklopčić, A. & Hirata, C. M. 2018, ApJ Letters, 855, L11
Öpik, E. J. 1963, Geophysical Journal, 7, 490
Orell-Miquel, J., Murgas, F., Pallé, E., et al. 2022, A&A, 659, A55
Owen, J. E. & Alvarez, M. A. 2016, ApJ, 816, 34
Owen, J. E. & Lai, D. 2018, MNRAS, 479, 5012
Owen, J. E., Murray-Clay, R. A., Schreyer, E., et al. 2021, arXiv e-prints, arXiv:2111.06094
Owen, J. E. & Wu, Y. 2013, ApJ, 775, 105
Palle, E., Nortmann, L., Casasayas-Barris, N., et al. 2020, A&A, 638, A61
Paragas, K., Vissapragada, S., Knutson, H. A., et al. 2021, ApJ Letters, 909, L10
Parker, E. N. 1958, ApJ, 128, 664
Pillitteri, I., Micela, G., Maggio, A., Sciortino, S., & Lopez-Santiago, J. 2022, A&A, 660, A75
Poppenhaeger, K. 2022, MNRAS, 512, 1751
Rackham, B. V., Apai, D., & Giampapa, M. S. 2019, AJ, 157, 96
Rackham, B. V., Espinoza, N., Berdyugina, S. V., et al. 2022, arXiv e-prints, arXiv:2201.09905
Ridden-Harper, A. R., Snellen, I. A. G., Keller, C. U., et al. 2016, A&A, 593, A129
Rockcliffe, K. E., Newton, E. R., Youngblood, A., et al. 2021, AJ, 162, 116
Salz, M., Czesla, S., Schneider, P. C., et al. 2018, A&A, 620, A97
Salz, M., Schneider, P. C., Czesla, S., & Schmitt, J. H. M. M. 2016, A&A, 585, L2
Sánchez-López, A., Lin, L., Snellen, I. A. G., et al. 2022, A&A, 666, L1
Schilling, G. 1996, Science, 273, 429
Schlawin, E., Agol, E., Walkowicz, L. M., Covey, K., & Lloyd, J. P. 2010, ApJ Letters, 722, L75
Seager, S. & Sasselov, D. D. 2000, ApJ, 537, 916

Sing, D. K., Fortney, J. J., Nikolov, N., et al. 2016, Nature, 529, 59
Sing, D. K., Lavvas, P., Ballester, G. E., et al. 2019, AJ, 158, 91
Spake, J. J., Oklopčić, A., & Hillenbrand, L. A. 2021, AJ, 162, 284
Spake, J. J., Oklopčić, A., Hillenbrand, L. A., et al. 2022, arXiv e-prints, arXiv:2209.03502
Spake, J. J., Sing, D. K., Evans, T. M., et al. 2018, Nature, 557, 68
Szabó, G. M. & Kiss, L. L. 2011, ApJ, 727, L44
Tripathi, A., Kratter, K. M., Murray-Clay, R. A., & Krumholz, M. R. 2015, ApJ, 808, 173
Vidal-Madjar, A., Désert, J.-M., Lecavelier des Etangs, A., et al. 2004, ApJ Letters, 604, L69
Vidal-Madjar, A., Huitson, C. M., Bourrier, V., et al. 2013, A&A, 560, A54
Vidal-Madjar, A., Lecavelier des Etangs, A., Désert, J.-M., et al. 2003, Nature, 422, 143
Vidotto, A. A. & Bourrier, V. 2017, MNRAS, 470, 4026
Villarreal D'Angelo, C., Vidotto, A. A., Esquivel, A., Hazra, G., & Youngblood, A. 2021, MNRAS, 501, 4383
Vissapragada, S., Knutson, H. A., Greklek-McKeon, M., et al. 2022, arXiv e-prints, arXiv:2204.11865
Vissapragada, S., Knutson, H. A., Jovanovic, N., et al. 2020, AJ, 159, 278
Vissapragada, S., Stefánsson, G., Greklek-McKeon, M., et al. 2021, AJ, 162, 222
Volkov, A. N., Johnson, R. E., Tucker, O. J., & Erwin, J. T. 2011, ApJ Letters, 729, L24
Waalkes, W. C., Berta-Thompson, Z., Bourrier, V., et al. 2019, AJ, 158, 50
Wang, L. & Dai, F. 2018, ApJ, 860, 175
Watson, A. J., Donahue, T. M., & Walker, J. C. G. 1981, Icarus, 48, 150
Wyttenbach, A., Ehrenreich, D., Lovis, C., Udry, S., & Pepe, F. 2015, A&A, 577, A62
Wyttenbach, A., Mollière, P., Ehrenreich, D., et al. 2020, A&A, 638, A87
Yan, D., Guo, J., Huang, C., & Xing, L. 2021a, ApJ Letters, 907, L47
Yan, F. & Henning, T. 2018, Nature Astronomy, 2, 714
Yan, F., Wyttenbach, A., Casasayas-Barris, N., et al. 2021b, A&A, 645, A22
Zhang, M., Cauley, P. W., Knutson, H. A., et al. 2022a, arXiv e-prints, arXiv:2204.02985
Zhang, M., Knutson, H. A., Dai, F., et al. 2022b, arXiv e-prints, arXiv:2207.13099
Zhang, M., Knutson, H. A., Wang, L., Dai, F., & Barragán, O. 2022c, AJ, 163, 67
Zhang, M., Knutson, H. A., Wang, L., et al. 2022d, AJ, 163, 68
Zhang, M., Knutson, H. A., Wang, L., et al. 2021, AJ, 161, 181
Zhang, Y., Snellen, I. A. G., Mollière, P., et al. 2020, A&A, 641, A161

https://doi.org/10.1017/S1743921322004239 Published online by Cambridge University Press